Table 1 Products of the fluorination of CH_2Cl_2

	Mass of metal fluoride/g	Mass of CH_2Cl_2/g	Products[b] (mol%)									Inorganic residue
			CH_2ClF	CH_2F_2	$CHCl_2F$	$CHClF_2$	CHF_3	CF_2Cl_2	CF_3Cl	CF_4	HF	
ReF_7	0.2073	1.0613	1.40	—	48.66	0.64	—	—	—	—	49.30	ReF_6
ReF_6	0.0322	0.4757	82.44	3.32	3.98	3.14	—	—	—	—	7.12	'$ReCl_3F_3$'
OsF_6	0.0379	0.2360	21.86	54.14	—	1.31	7.83	0.26	1.65	—	12.95	$OsCl_5$
IrF_6	0.0392	0.1896	32.63	22.77	8.62	7.93	5.75	—	—	—	22.30	'$IrCl_3$'
UF_6	0.4150	1.3175	—	—	49.95	—	—	—	—	—	49.95	β-UF_5
RuF_5	0.0608	0.6472	36.18	57.09	1.62	1.12	0.62	—	—	—	3.36	'$RuCl_3$'
VF_5	0.1905	0.9425	0.98	—	46.40	3.11	—	—	—	—	49.51	VF_3
CrF_5[a]	0.2054	2.0868	27.84	2.58	8.17	27.54	3.02	2.00	2.38	4.42	—	CrF_4

[a] Reaction performed in HF (0.6858 g, 34.289 mmol) (see text). [b] Mol %.

Indeed, although ReF_7 undergoes relatively fast (*ca.* 4 h) hydrogen–fluorine exchange, ReF_6 (produced as the initial byproduct of the ReF_7 reduction) undergoes a slow (more than 5 days) chlorine–fluorine exchange. There is an increase in reactivity ($ReF_6 < OsF_6 < IrF_6$) for reactions with both dichloromethane and inorganic chlorides; the inorganic products are the same from both types of reaction. There is also a decrease in specificity for Cl–F exchange in this series as a consequence of the extreme reactivity of the Os^{VI} and Ir^{VI} species. The critical role of the metal d^n configuration and the mechanisms of these reactions are unclear at present. The absence of $CHCl_3$ and CCl_4 indicates that the reactions do not involve organic radicals and suggests a concerted mechanism with coordination of the dichloromethane to the very electron deficient metal centres. Further work into the mechanisms of these unusual reactions and the fluorination of other organic molecules by high oxidation state transition metal fluorides is in progress.

We would like to thank ICI Chemical and Polymers Ltd. (W. W. D., M. R. R.) and the SERC (W. W. D., E. G. H., P. J. T.) for financial support.

Received, 2nd June 1993; Com. 3/03117I

References

1 W. W. Dukat, J. H. Holloway, E. G. Hope, M. R. Rieland, P. J. Townson and R. L. Powell, Eur. Pat. Appl., 92301531.7, 1992.
2 See for example, R. E. Banks and J. C. Tatlow, *J. Fluorine Chem.*, 1986, **33**, 267.
3 G. A. Olah, J. G. Shih and G. K. S. Prakash, *J. Fluorine Chem.*, 1986, **33**, 385.
4 G. A. Olah, J. Welch, G. K. S. Prakash and T. L. Ho, *Synthesis*, 1976, 808.
5 G. A. Olah and J. Welch, *Synthesis*, 1976, 809.
6 V. V. Bardin, A. A. Avramenko, G. G. Furin, G. G. Yakobson, V. A. Krasilnikov, P. P. Tushin and A. I. Karelin, *J. Fluorine Chem.*, 1985, **28**, 37.
7 H. C. Clarke and H. J. Emeléus, *J. Chem. Soc.*, 1957, 2119.
8 R. C. Burns and T. A. O'Donnell, *Inorg. Chem.*, 1979, **18**, 3081.
9 J. H. Holloway, G. Stanger, E. G. Hope, W. Levason and J. S. Ogden, *J. Chem. Soc., Dalton Trans.*, 1988, 1341; A. K. Brisdon, P. J. Jones, W. Levason, J. S. Ogden, J. H. Holloway, E. G. Hope and G. Stanger, *J. Chem. Soc., Dalton Trans.*, 1990, 715; A. K. Brisdon, J. H. Holloway, E. G. Hope, W. Levason, J. S. Ogden and A. K. Saad, *J. Chem. Soc., Dalton Trans.*, 1992, 139; 447.
10 T. A. O'Donnell and D. F. Stewart, *Inorg. Chem.*, 1966, **5**, 1434; G. W. Fraser, M. Mercer and R. D. Peacock, *J. Chem. Soc.*, 1967, 1091; G. W. Fraser, C. J. W. Gibbs and R. D. Peacock, *J. Chem. Soc.*, (*A*), 1970, 1708.

Silver Zeolite 4A Modified Electrodes: Intrazeolite Effect

Jian-wei Li and Gion Calzaferri*

Institute for Inorganic and Physical Chemistry, University of Berne, Freiestrasse 3, CH-3000 Berne 9, Switzerland

The cyclic voltammograms of Ag^+-exchanged zeolite A as a monograin layer on glassy carbon electrodes show a dramatic dependence on the degree of exchange and indicate that the silver ions in the zeolite are electrochemically 'active'.

All kinds of spectroscopic techniques have been applied for characterizing silver zeolites but only a few studies have been devoted to electrochemical characteristics of zeolite-modified electrodes containing silver ions.[1–3] We have found recently that electrodes modified with a dense monograin zeolite layer are well suited for electrochemical studies[4] and we now describe the voltammetric behaviour of silver zeolite A, $Ag_xNa_{12-x}(AlO_2)_{12}(SiO_2)_{12}$, for different degrees of exchange x. To understand the operation of zeolite electrodes, it is important to distinguish between responses originating from the surface and the interior of the zeolite. For this reason extra- and intra-zeolite electrochemical processes will be discussed.

A 3 mm diameter glassy carbon disk electrode with Teflon sheathing was polished with 0.3 μm Al_2O_3, washed ultrasonically in water three times and electrolysed in 0.1 mol l^{-1} $LiClO_4$ at a rotation frequency of 3000 rpm by holding the potential at 0.9 V *vs.* saturated calomel electrode (SCE) for 5 min, and then washed thoroughly with doubly distilled water. 5 μl of zeolite dispersion [60 mg of zeolite Na_{12}-A (Linde 4A, Baylith T, Bayer) in 15 ml of H_2O, 1 h sonication before use] was dropped on the surface of the electrode. After slowly drying at room temp., 5 μl of polystyrene solution [3 mg of polystyrene in 25 ml of tetrahydrofuran (THF)] was dropped on the zeolite layer and evaporated at room temp. The coating obtained contains 20 μg of zeolite and 0.6 μg of

polystyrene and consists of one monograin layer as analysed by scanning electron microscopy (SEM). The mechanical stability of this layer is high; no apparent loss of zeolite from the surface of the glassy carbon electrode rotating at 3000 rpm in aqueous solution has been observed. Before use in cyclic voltammetry,† the modified electrodes were cleaned with rotation at 500 rpm in 0.1 mol l^{-1} $NaNO_3$ for 10 min, then ion-exchanged in the dark with rotation at 500 rpm in $NaNO_3$ + $AgNO_3$ solutions with different Ag^+/Na^+ ratios for different Ag^+-exchange degrees, and finally washed thoroughly in doubly distilled water. Cyclic voltammograms were measured at different scan rates immediately after immersion of the electrodes into the electrolyte. The cyclic voltammograms measured at 5 mV s^{-1} for electrodes with different degrees of exchange x of 2.6, 4.0, 6.5 and 12 are shown in Fig. 1. The reproducibility of these results was checked by carrying out all experiments three times. The integrated area of the first cathodic wave was the same within ±5%. This indicates that the experimental procedure is reproducible and that the zeolite layer on the glassy carbon electrode is stable.

About 85% of the silver ions in the zeolite are electrochemically reduced at this scan rate during the first cathodic scan for all degrees of exchange investigated. A dramatic dependence of the peaks and shoulders on the degree of exchange x is apparent in Fig. 1. This indicates the presence of eight electrochemically distinct silver species, which we denote as A, B, C, D, E, F, G and H, respectively. We first note that the peak potential of the peak H matches exactly the peak potential of reduction of silver ions on the same blank glassy carbon electrode under otherwise identical conditions. It is caused by diffusion of Ag^+ ions from the zeolite to the surface of the glassy carbon electrode and reduction during the cathodic scan. Because the degree and the rate of this process depend on the initial Ag^+-exchange degree x, this peak appears only in the fully Ag^+-exchanged sample, x = 12. Baker and Zhang[3] have explained the voltammetric behaviour of their silver zeolite Y modified electrodes by assuming that Ag^+ ions located at two different sites in zeolite Y possess different redox abilities. In fully hydrated silver zeolite A, the Ag^+ ions are located at four different sites. It was reported that the least strongly coordinated silver ions are reduced first.[5]

We have observed seven electrochemically distinct species (A–G) in addition to H, however, and found that the appearance of them strongly depends on x, a fact that has not hitherto been reported. To explain these observations, further assumptions have to be made. First, the silver ions prefer the sites in the zeolite to which they are most strongly coordinated. Secondly, the reduced Ag^0 atoms react with each other and with unreduced Ag^+ ions to form uncharged and charged silver clusters, Ag_n^{m+} ($m < n$), the sizes of which are limited by the sizes of the zeolite cages. These clusters possess different redox abilities.[6,7]

We conclude that at low Ag^+-exchange degrees, the Ag^+ ions are mainly located at sites at which it is more difficult for them to be reduced and smaller clusters are formed as compared with high Ag^+-exchange degrees. The electrodes respond in the more negative potential region in this case. With increasing Ag^+ concentration, more and more Ag^+ ions occupy sites at which they are easily reduced and larger clusters are formed as compared with low Ag^+-exchange degrees. As a result, the electrode responds in the more positive potential region. This means that the seven peaks and shoulders (A–G) are caused not only by site-effects, but also by the formation of silver clusters of different size which depends on the initial concentration of Ag^+ ions in the zeolite.

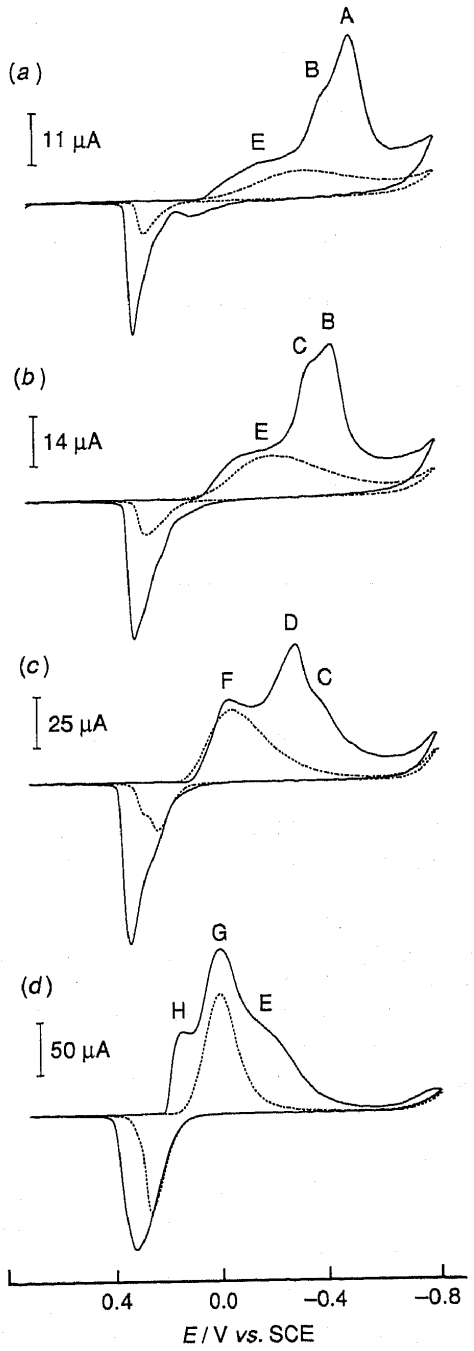

Fig. 1 Cyclic voltammograms of silver zeolite 4A modified electrodes in 0.1 mol l^{-1} $LiClO_4$ at 20 °C at a scan rate of 5 mV s^{-1}. The initial potential is 0.7 V and the switching potential is −0.8 V. The upper half of traces are the cathodic currents. (*a*), (*b*), (*c*) and (*d*) illustrate measurements at different degrees of silver ion-exchange, namely x = 2.6, 4.0, 6.5 and 12. Solid lines are the first cycles and dashed lines are the second cycles. SCE = saturated calomel electrode.

What is the reason for the dramatic decreases of the current in the second cycles? This decreases faster at low x than at high x, and, as mentioned above, nearly the same percentage (about 85%) of Ag^+ ions in the zeolite are reduced during the first cathodic scan for all degrees of exchange. This can be explained by assuming that the decrease of the current during the second cycle is mainly caused by migration of uncharged silver clusters out of the zeolite framework and growth on the surface of the zeolite to form electrochemically 'silent' silver particles.[4,9] Provided that the smaller uncharged silver clusters migrate faster than the larger ones,[8] the current of the second cycle is expected to decrease faster at low exchange degree.

† One-compartment, three-electrode cell with a water jacket for connection to a constant-temperature circulator; Pt sheet counter electrode and saturated calomel reference electrode with a 1 mol l^{-1} $NaNO_3$ bridge electrolyte solution with Vycor frit to avoid the influence of Cl^- ions; EG&G model 273 potentiostat and model 270 electrochemical analysis system; $LiClO_4$ (0.1 mol l^{-1}) (Merck, p.a.) Ar-purged supporting electrolyte solution; no *IR* compensation.

All explanations given in this paper are also supported by the observed influence of the scan rate (0.5 to 50 mV s^{-1}) on cyclic voltammograms. We conclude that the cathodic reduction of silver ions in the zeolite A is dominated by intrazeolite processes.

This work is part of project NF 20-28528.90, financed by the Schweizerische Nationalfonds zur Föderung der wissenschaftlichen Forschung and project BEW-EPA 217.307, financed by the Schweizerische Bundesamt für Energiewirtschaft.

Received, 11th May 1993; Com. 3/02658B

References

1 D. R. Rolinson, *Chem. Rev.*, 1990, **90**, 867.
2 J.-P. Pereira-Ramos, R. Messina and J. Perichon, *J. Electroanal. Chem.*, 1983, **146**, 157.
3 M. D. Baker and J. Zhang, *J. Phys. Chem.*, 1990, **94**, 8703.
4 G. Calzaferri, K. Hädener and J. Li, *J. Chem. Soc., Chem. Commun.*, 1991, 653.
5 Y. Kim and K. Seff, *J. Phys. Chem.*, 1978, **82**, 1071.
6 G. Calzaferri, Proceedings IPS-9, Beijing, ed. Z. W. Tian and Y. Cao, International Academic Publishers, 1993, 141; R. Beer, G. Calzaferri, J. Li and B. Waldeck, *Coord. Chem. Rev.*, 1991, **111**, 193.
7 T. Baba, N. Akinaka, M. Nomura and Y. Ono, *J. Chem. Soc., Faraday Trans.*, 1993, **89**, 595; J. Amblard, O. Platzer, J. Ridard and J. Belloni, *J. Phys. Chem.*, 1992, **96**, 2341; A. Henglein, *Ber. Bunsenges. Phys. Chem.*, 1990, **94**, 600; W. J. Plieth, *J. Phys. Chem.*, 1982, **86**, 3166.
8 Y. Kim and K. Seff, *Bull. Korean Chem. Soc.*, 1987, **8**, 69.
9 Y. Kim and K. Seff, *J. Phys. Chem.*, 1987, **91**, 668.

Carbonyl Insertion and Reductive Elimination Chemistry of Tungsten(II) Alkoxides and Aryloxides

Brian P. Buffin, Atta M. Arif and Thomas G. Richmond*

Department of Chemistry, University of Utah, Salt Lake City, Utah 84112, USA

Carbonyl insertion into the W–O bond in a series of novel W^{II} alkoxides and aryloxides, containing a tridentate monoanionic [C,N,N'] ligand, results in the generation of alkoxycarbonyl- and aryloxycarbonyl-groups, which readily reductively eliminate to form new C–C bonds; in contrast, carbon dioxide insertion into the W–OMe alkoxide bond generates an η^1-carbonate ligand, which retains coordination to the metal centre.

The activation of small molecules by transition metal alkoxides has received renewed attention in recent years owing, in part, to their proposed role in several important homogeneous reactions including the catalytic carbonylation of methanol by tungsten hexacarbonyl/potassium methoxide[1] and the reduction of organic carbonyls.[2] Although the chemistry of group 6 metal alkoxides has been extensively studied in d^6 anionic complexes of $[M(CO)_5OR]^-$,[3] bimetallic d^3–d^3 systems,[4] and higher oxidation state complexes,[5] little has been reported on d^4 M^{II} alkoxides and aryloxides.[6] The stabilization of hard ligands such as fluoride by monoanionic [C,N,N'] chelating ligands at tungsten(II)[7] suggests that related metal alkoxides could be prepared.† In this work we report the synthesis and reactivity of a series of novel W^{II} alkoxides and aryloxides, which are found to be stable to decomposition pathways such as β-hydrogen elimination and exhibit interesting insertion chemistry.

As shown in Scheme 1,‡ treatment of the tungsten(II) bromide **1**, which can be readily prepared by the room temperature oxidative addition reaction of the chelating arylbromide ligand with $W(CO)_3(EtCN)_3$,[8] with silver trifluoromethanesulfonate results in quantitative spectroscopic conversion to the tungsten(II) triflate **2**, which can be isolated as an air-stable yellow solid in 86% yield from CH_2Cl_2. The increase in IR carbonyl stretching frequencies upon halide exchange is indicative of the weak donor ability of the trifluoromethanesulfonate anion. Addition of sodium alkoxide or aryloxide salts to a tetrahydrofuran (THF) solution of **2** results in displacement of the labile triflate ligand and a quantitative spectroscopic conversion to the corresponding tungsten(II) alkoxides **3**,**5** and aryloxide **4**, which were isolated as air-stable, yellow solids in 70–84% yields. The methoxide complex **3** was further characterized by X-ray crystallography§ as illustrated in Fig. 1. The geometry about the seven-coordinate tungsten atom is best described as capped octahedral with the *ipso*-carbon C(4) of the phenyl ring capping the trigonal face comprised of N(1), C(1), and C(2). The bent methoxide ligand has a W–O(4)–C(16) bond angle of 125.6(5)° as expected with a W–O(4) distance of 2.033(5) Å, which is intermediary between that observed for the d^6 $[W(CO)_5OPh]^-$ anion of 2.18(2) Å[3a] and that of the d^2

† To our knowledge Group 6 d^4 complexes such as $CpM(CO)_3OR$ (where M = Cr, Mo, or W and R = Me, Et, or Ph) have yet to be prepared.

‡ All new compounds were characterized by IR, ^1H, ^{13}C, and ^{19}F NMR spectroscopic methods and satisfactory elemental analyses (C,H,N) were obtained. *Selected spectroscopic data*: **2**: IR ν_{CO} 2020m, 1931s, 1895m cm^{-1}. **3**: IR ν_{CO} 1991m, 1895s, 1860m cm^{-1}; ^{13}C NMR (CD_2Cl_2) δ COs 227.0, *ipso*-C 150.8, OCH_3 64.33. **6**: IR ν_{CO} 2007m, 1873s, 1863vs, 1837s, 1722w cm^{-1}; ^{13}C NMR ($CDCl_3$) δ COs 213.3, 213.1, 206.2, 206.1, *C*(O)OMe 168.3, OCH_3 52.65. **9**: IR ν_{CO} 2010m, 1917s, 1881m, 1694w, 1276w cm^{-1}; ^{13}C NMR (CD_2Cl_2) δ COs 224.9, *ipso*-C 147.0, *O*C(O)OMe 159.8, OCH_3 53.94. All IR data obtained in THF.

§ *Crystallographic data* for **3** ($C_{16}H_{22}N_2O_4W$): Monoclinic space group $P2_1/c$, a = 13.568(3), b = 8.655(3), c = 15.746(3) Å, β = 105.90(2)°, V = 1778.3 $Å^3$, and Z = 4 based on 2724 observations at 18 °C (Mo-Kα, 4°<2θ<50°, μ = 66.544 cm^{-1}, empirical absorption correction applied) with $I>3\sigma(I)$ and 208 variables to yield R = 0.0259, R_w = 0.0327, and GOF = 1.17.

Atomic coordinates, bond lengths and angles, and thermal parameters have been deposited at the Cambridge Crystallographic Data Centre. See Notice to Authors, Issue No. 1.